Rotational relaxation of HCO+ and DCO+ by collision with H2

Otoniel Denis-Alpizar, Thierry Stoecklin, Anne Dutrey, Stéphane Guilloteau

▶ **To cite this version:**

Otoniel Denis-Alpizar, Thierry Stoecklin, Anne Dutrey, Stéphane Guilloteau. Rotational relaxation of HCO+ and DCO+ by collision with H2. Monthly Notices of the Royal Astronomical Society, 2020, 497 (4), pp.4276 - 4281. 10.1093/mnras/staa2308 . hal-03044185

HAL Id: hal-03044185

https://cnrs.hal.science/hal-03044185

Submitted on 16 Dec 2020

HAL is a multi-disciplinary open access archive for the deposit and dissemination of scientific research documents, whether they are published or not. The documents may come from teaching and research institutions in France or abroad, or from public or private research centers.

L'archive ouverte pluridisciplinaire **HAL**, est destinée au dépôt et à la diffusion de documents scientifiques de niveau recherche, publiés ou non, émanant des établissements d'enseignement et de recherche français ou étrangers, des laboratoires publics ou privés.

Distributed under a Creative Commons Attribution 4.0 International License

Monthly Notices of the ROYAL ASTRONOMICAL SOCIETY

MNRAS **497,** 4276–4281 (2020) doi:10.1093/mnras/staa2308
Advance Access publication 2020 August 5

Rotational relaxation of HCO^+ and DCO^+ by collision with H_2

Otoniel Denis-Alpizar [1]★ Thierry Stoecklin,[2] Anne Dutrey[3] and Stéphane Guilloteau[3]

[1]*Núcleo de Astroquímica y Astrofísica, Instituto de Ciencias Químicas Aplicadas, Facultad de Ingeniería, Universidad Autónoma de Chile, Av. Pedro de Valdivia 425, 7500912 Providencia, Santiago, Chile*
[2]*Institut des Sciences Moléculaires, Université de Bordeaux, CNRS UMR 5255, F-33405 Talence Cedex, France*
[3]*Laboratoire d'Astrophysique de Bordeaux, Université de Bordeaux, CNRS, B18N, Allée Geoffroy Saint-Hilaire, F-33615 Pessac, France*

Accepted 2020 July 31. Received 2020 July 31; in original form 2020 June 8

ABSTRACT

The HCO^+ and DCO^+ molecules are commonly used as tracers in the interstellar medium. Therefore, accurate rotational rate coefficients of these systems with He and H_2 are crucial in non-local thermal equilibrium models. We determine in this work the rotational de-excitation rate coefficients of HCO^+ in collision with both *para*- and *ortho*-H_2, and also analyse the isotopic effects by studying the case of DCO^+. A new four-dimensional potential energy surface from ab initio calculations was developed for the HCO^+–H_2 system, and adapted to the DCO^+–H_2 case. These surfaces are then employed in close-coupling calculations to determine the rotational de-excitation cross-sections and rate coefficients for the lower rotational states of HCO^+ and DCO^+. The new rate coefficients for $HCO^+ + para$-H_2 were compared with the available data, and a set of rate coefficients for $HCO^+ + ortho$-H_2 is also reported. The difference between the collision rates with *ortho*- and *para*-H_2 is found to be small. These calculations confirm that the use of the rate coefficients for $HCO^+ + para$-H_2 for estimating those for $HCO^+ + ortho$-H_2 as well as for $DCO^+ + para$-H_2 is a good approximation.

Key words: astrochemistry – molecular data – molecular processes – scattering – ISM: molecules.

1 INTRODUCTION

Although molecular cloud temperatures can range from 5 K up to a few tens of K, and densities from 10^2 up to 10^6 cm^{-3}, the temperature and densities of most molecular clouds are low, 10–15 K and 10^2–10^4 cm^{-3}, respectively, and therefore, the collisions are rare. As a result, the rotational population of molecules in these regions cannot be described by a Boltzmann distribution. The physico-chemical conditions in the molecular clouds should be determined then by non-local thermal equilibrium (non-LTE) models. Such models require not only the knowledge of the Einstein coefficients, usually known, but also the state-to-state rate coefficients of the observed molecule with the most common colliders in the interstellar medium (ISM), named H_2, He, e, and H.

HCO^+, discovered by Buhl & Snyder (1970), was the first cation identified in the cold ISM (Kraemer & Diercksen 1976). It has been detected almost in all the regions of the ISM, including dense cores, molecular outflows, and even diffuse clouds (Lucas & Liszt 1996). Its deuterated species, DCO^+, is also considered as one of the primary tracers of the deuterium chemistry in the ISM (Huang et al. 2017). HCO^+ and DCO^+ are often used as tracers of ionization in dense cores (Caselli et al. 1998) and DCO^+ is easily observed in the molecular layer of protoplanetary discs (e.g. Dutrey et al. 2014). Accurate rate coefficients of these systems with He and H_2 are thus important for a correct description of the physico-chemical conditions in these astrophysical media.

The rotational rate coefficients of HCO^+ with He were reported by Buffa, Dore & Meuwly (2009). For the collision of HCO^+ with H_2, the first set of rate coefficients was computed by Monteiro (1985) from a potential energy surface (PES) determined at the self-consistent field (SCF) level of theory and limited to low temperatures ($T \leq 30$ K) and the lower rotational states. The data that can be found in the LAMDA (Schöier et al. 2005) and BASECOL (Dubernet et al. 2013) data bases are those reported by Flower (1999), who extended the calculations of Monteiro (1985). However, such rate coefficients were computed using the same PES. More recently, Yazidi, Ben Abdallah & Lique (2014) calculated a new set of rate coefficients for the lower 21 transitions of HCO^+ from a PES averaged over the H_2 orientation. Such data showed significant differences with the rate coefficients of Flower (1999). The use of the averaged PES in the determination of the rate coefficients was validated by the calculations of Massó & Wiesenfeld (2014). These authors employed a four-dimensional PES for the HCO^+–H_2 complex at a high level of theory and computed the cross-section and rate coefficients for the lower states of HCO^+. However, all available sets of rate coefficients, large enough for being included in non-LTE calculations, are restricted to the collision with *para*-H_2. The only study that considered the collision with *ortho*-H_2 was limited to the three lower rotational states of HCO^+ (Massó & Wiesenfeld 2014). Therefore, a large set of rate coefficients for the collision of HCO^+ with *ortho*-H_2 deserves to be computed.

The case of DCO^+ is quite different. Its collision with He was also studied (Buffa 2012), and differences of about 20 per cent were found between the rate coefficients of $HCO^+ + He$ and $DCO^+ + He$. However, there is no set of rate coefficients for its collision with

★ E-mail: otoniel.denis@uautonoma.cl

© 2020 The Author(s)
Published by Oxford University Press on behalf of the Royal Astronomical Society

Downloaded from https://academic.oup.com/mnras/article/497/4/4276/5881339 by guest on 28 September 2020

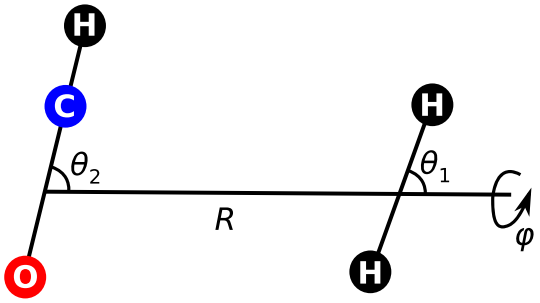

Figure 1. Internal coordinates used to describe the HCO$^+$ + H$_2$ system. The azimuthal angle φ is undefined when θ_1 or θ_2 is equal to 0° or 180°.

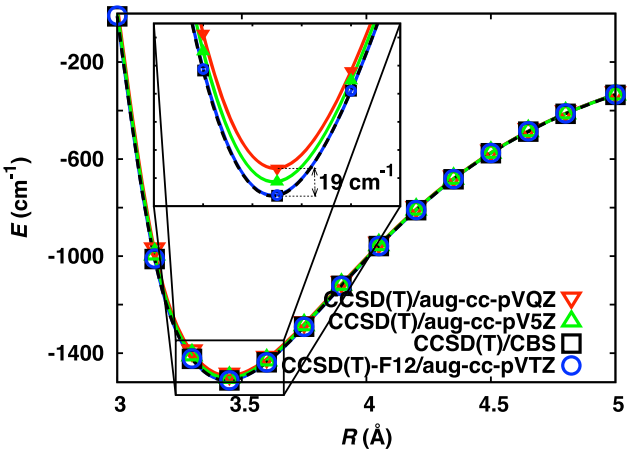

Figure 2. Ab initio energies computed at the CCSD(T)-F12a/aug-cc-pVTZ, CCSD(T)/aug-cc-pVQZ, and CCSD(T)/aug-cc-pV5Z level of theory and those extrapolated to the CBS limit, at $\theta_1 = 90°$ and $\theta_2 = 0°$.

H$_2$. Pagani, Bourgoin & Lique (2012) estimated the hyperfine rate coefficients for DCO$^+$ + H$_2$ but using the rate coefficients for HCO$^+$ + H$_2$ and ignoring the isotopic substitution of HCO$^+$. In the main data bases for collisional data, namely LAMDA (Schöier et al. 2005) and BASECOL (Dubernet et al. 2013), the rate coefficients for DCO$^+$ + H$_2$ are assumed to be the same as for HCO$^+$ + H$_2$, and astronomers usually employ these rate coefficients in the non-LTE models used to analyse the observations of DCO$^+$. However, in the case of the isoelectronic molecule HCN in collision with He, the ratio between the rate coefficients for both isotopologues, namely HCN and DCN, varies from 0.4 to 3.9 (Denis-Alpizar, Stoecklin & Halvick 2015). This approximation used for DCO$^+$ thus deserves to be checked.

The main goal of this work is to determine the first set of rotational de-excitation rate coefficients of HCO$^+$ in collision with both *para*- and *ortho*-H$_2$ that can be used in non-LTE models from a four-dimensional PES, also developed in this work. Furthermore, this PES will be modified to describe the DCO$^+$ + H$_2$ system, and the dynamics of DCO$^+$ + H$_2$ will also be studied. This paper is organized as follows: In the next section, the methods employed are described, while the results are analysed in Section 3. Finally, the summary of this work is provided in Section 4.

2 METHODS

2.1 Ab initio calculations

The HCO$^+$ + H$_2$ complex was described employing the coordinates shown in Fig. 1, where R connects the centres of mass of the H$_2$ and HCO$^+$ molecules and θ_1, θ_2, and φ describe the relative angular orientations. The HCO$^+$ and H$_2$ molecules were considered as rigid rotors. The use of this approximation has allowed an excellent prediction of experimental results for several molecule–diatom collisions, e.g. O$_2$–H$_2$ (Lique et al. 2014) and CO–D$_2$ (Stoecklin et al. 2017). Furthermore, recent close-coupling calculations considering the bending motions for the collision with a triatomic system have shown that the rigid rotor approximation is valid for collisional energies lower than the bending frequency (Stoecklin et al. 2013; Denis-Alpizar, Stoecklin & Halvick 2014; Denis-Alpizar et al. 2015). The bond length of H$_2$ was taken as the vibrationally averaged value in the rovibrational ground state $r_{\rm H-H} = 0.767$ Å (Jankowski & Szalewicz 1998), while for the linear HCO$^+$ molecule, the CO and CH distances were set to the experimental equilibrium values $r_{\rm CO} = 1.105$ Å and $r_{\rm CH} = 1.097$ Å (Woods 1988).

The ab initio calculations were performed at the explicitly correlated coupled-cluster level, including single, double, and perturbative triple excitations [CCSD(T)-F12a] using the MOLPRO package (Werner et al. 2012). In such method, the direct inclusion of F12 terms in the triples is not available, and an improvement of the energy of the triples was obtained by scaling the triples' energy contribution (Knizia, Adler & Werner 2009) as implemented in MOLPRO (Werner et al. 2012). This correction gives energies close to the completed basis set (CBS) limit for the augmented correlation-consistent polarized triple zeta basis set (aug-cc-pVTZ) of Dunning (1989) (Knizia et al. 2009). Therefore, the aug-cc-pVTZ basis set was then employed in this work. The non-size consistency of the CCSD(T)-F12a method was corrected by shifting up the ab initio interaction energies to make it vanish at $R = 350$ Å. The basis set superposition error was corrected using the counterpoise procedure of Boys & Bernardi (1970). Fig. 2 shows the energies computed in the region of the minimum of the complex, and those employing the standard CCSD(T) method with the aug-cc-pVQZ and aug-cc-pV5Z basis sets. The two-point extrapolation formula $E_{\rm CBS} = \frac{E_X X^3 - E_Y Y^3}{X^3 - Y^3}$, where X and Y are the cardinality of the basis set ($X = 5$ for aug-cc-pV5Z and $Y = 4$ for aug-cc-pVQZ; Halkier et al. 1999), was used for obtaining the energies at the CBS limit. The agreement of the energies computed with the CCSD(T)-F12a/aug-cc-pVTZ method and those at the CBS limit is excellent.

In total, 49 038 ab initio energies were computed. The radial grid includes 29 values of R from 1.8 to 20.0 Å, while θ_1 and θ_2 vary from 0° to 180° in steps of 15°. The azimuthal angle φ varies in steps of 20° in the [0, 180]° interval.

2.2 Analytical PES

The ab initio energies were fitted to the analytical function with the form

$$V(R,\theta_1,\theta_2,\varphi) = \sum_{l_1=0}^{4}\sum_{l_2=0}^{10}\sum_{m=0}^{\min(l_1,l_2)} f_m^{l_1,l_2}(R) \times \bar{P}_{l_1}^m(\cos\theta_1)\bar{P}_{l_2}^m(\cos\theta_2)\cos(m\varphi), \quad (1)$$

where the angular part is represented by a product of normalized associated Legendre functions and a cosine function. Only even values of l_1 are included in this function due to the symmetry of H$_2$. For each value of R, the ab initio energies were fitted using a least-square method. The coefficients $f_m^{l_1,l_2}$ were fitted using the Reproducing Kernel Hilbert Space procedure (Ho & Rabitz 1996)

Downloaded from https://academic.oup.com/mnras/article/497/4/4276/5881339 by guest on 28 September 2020

Table 1. Rotational de-excitation cross-sections (in a_0^2) of HCO^+ by collision with *para*-H_2 using one ($j_{H_2} = 0$) and two ($j_{H_2} = 0, 2$) rotational states of H_2 in the calculations at the collisional energies of 10 and 200 cm^{-1} for selected transitions.

HCO^+ states		$E = 10$ cm^{-1}		$E = 200$ cm^{-1}	
$j_{initial}$	j_{final}	$j_{H_2} = 0$	$j_{H_2} = 0, 2$	$j_{H_2} = 0$	$j_{H_2} = 0, 2$
4	3	398.5	425.1	87.1	94.5
4	2	378.1	334.4	34.0	38.6
4	1	207.3	186.3	22.1	19.6
4	0	80.7	62.5	6.2	5.4
5	4	368.1	430.8	86.7	89.7
5	3	323.9	375.0	39.1	40.8
5	2	221.5	211.9	25.9	26.6
5	1	160.0	132.9	13.0	13.8
5	0	46.7	53.9	6.9	6.4

by

$$f_m^{l_1,l_2}(R) = \sum_{k=1}^{N} \alpha_k^{l_1,l_2,m} q^{2,2}(R, R_k), \quad (2)$$

where N is the number of radial points of the grid R_k. The $q^{2,2}(R, R_k)$ is the one-dimensional kernels defined by Ho & Rabitz (1996), which ensures the long-range R^{-3} behaviour (Soldán & Hutson 2000). The $\alpha_k^{l_1,l_2,m}$ coefficients were found by solving the system of linear equations $\mathbf{q}(\mathbf{R}_i, \mathbf{R}_j)\alpha = \mathbf{f}_m^{l_1,l_2}(\mathbf{R}_i)$, where i and j label the different radial geometrical configuration of the grid.

2.3 Scattering

The dynamics was performed with the DIDIMAT code (Guillon et al. 2008) employing the explicitly correlated four-dimensional PES developed in this work. In this code, the close-coupling equations were solved in the space-fixed frame using the log-derivative propagator (Manolopoulos 1988) for collisional energies from 10^{-2} up to 1000 cm^{-1}. The rotational constants of H_2 were fixed to $B_{H_2} = 60.853$ cm^{-1} and for HCO^+ this value was $B_{HCO^+} = 1.4875$ cm^{-1}. The minimum propagation distance used was 50 a_0, and the convergence was checked as a function of the total angular momentum and maximum propagation distance for each collision energy.

The basis set used in the close-coupling calculations included 32 rotational states of HCO^+. Table 1 shows the influence of the number of rotational states of H_2 included in the basis set. At 10 cm^{-1}, and for the largest Δj transitions, differences can seem to be relatively large. They are, however, expected in this region where the resonances have the strongest effect on the magnitude of the cross-sections. In contrast, the agreement of the cross-sections at 200 cm^{-1}, which is still below the well depth, is much better as the contribution of the resonances in the magnitude of the cross-section is decreasing when the collision energy increases. Consequently, the effect of the limitation of the basis set of H_2 to its lowest rotational state only marginally affects the state-to-state rate coefficients as also found by Massó & Wiesenfeld (2014). Therefore, only one rotational state of H_2 was included in the basis set.

3 RESULTS

The large number of ab initio energies, together with the use of the least-square and kernel procedure, allows a fit of high quality. For negative energies, the root mean square error deviation (RMSD) is 1.99 $\times$ 10^{-2} cm^{-1}, while for energies in the interval $0 < E < 1000$ cm^{-1}, the RMSD is 7.78 $\times$ 10^{-2} cm^{-1}.

Fig. 3 shows the contour plots for the $HCO^+ + H_2$ complex at several configurations. The global minimum of the analytical PES, named -1509.35 cm^{-1}, was found at $R = 3.44$ Å, $\theta_1 = 90°$, and $\theta_2 = 0°$. This well is slightly deeper (1.46 per cent) than the one reported by Massó & Wiesenfeld (2014) (-1487.5 cm^{-1}), which was found at the same angular configuration and $R = 3.49$ Å. Such a small different value in the minimum of the PES arises from the fact that we used the explicitly correlated CCSD(T)-F12a method instead of the standard CCSD(T) used by Massó & Wiesenfeld (2014). This value is also in good agreement with previous studies for the $HCO^+ + H_2$ complex. Bieske et al. (1995) found a value of -1443 cm^{-1} from the quadratic configuration interaction method, including single and double excitations with perturbative treatment of triples [QCISD(T)], while Li et al. (2008) reported a well of -1482 cm^{-1} computed with the CCSD(T) method. However, the PES from Monteiro (1985), computed only at the SCF level, and especially from Yazidi et al. (2014), that used a CCSD(T) PES averaged over the H_2 orientation exhibits much larger differences (-168 and -913 cm^{-1}, respectively). If our surface is averaged over the H_2 orientation, the global minimum (-971 cm^{-1}) is also deeper than the one of Yazidi et al. (2014), but shows similar anisotropy. This difference is because the basis set used by Yazidi et al. (2014) produces results comparable to the energies computed at the CCSD(T)/aug-cc-pVQZ level, while in our case the energies are close to the CBS limit, as can be seen from Fig. 2.

The PES previously presented was employed for determining the cross-sections for the lowest rotational states of HCO^+ (up to $j = 21$) in collision with both *para*- and *ortho*-H_2. The state-to-state rate coefficients were determined by the average of the corresponding cross-sections over a Maxwell–Boltzmann distribution of the collision energy.

The rotational rate coefficients computed here for $HCO^+ + H_2$ and those computed by Monteiro (1985), Flower (1999), Yazidi et al. (2014), and Massó & Wiesenfeld (2014) are shown in Table 2. The agreement with the calculations of Yazidi et al. (2014) is excellent. This is a new confirmation that the use of an averaged PES is a good approximation for studying the collision of a linear molecule with *para*-$H_2(j = 0)$. It is worth noting that the averaged PES approximation employed by Yazidi et al. (2014) transforms a four-dimensional PES to a two-dimensional surface by an average over the angular orientation of H_2, and the collision with *para*-$H_2(j = 0)$ is then treated as the scattering of a linear rigid rotor with an atom. This is justified because in the dynamics of the collision with *para*-$H_2(j = 0)$, the coupling matrix elements are non-zero only if $l_1 = 0$ (Cabrera-González, Páez-Hernández & Denis-Alpizar 2020). The main limitation of such approximation is that it is valid only for $H_2(j = 0)$.

Also, from Table 2, it can be seen that the rate coefficients for the collision with *para*- and *ortho*-H_2 are very close in magnitude. Fig. 4 shows the maximum percentage difference between both sets of rate coefficients at all $|\Delta j|$ considered in this work. The behaviour of the per cent difference is almost independent of the temperature, and even if it increases after $j = 13$, the values remain very close between them. The ratio between the rate coefficients for $HCO^+ +$ *ortho*-H_2 and $HCO^+ +$ *para*-H_2 varies from 0.75 up to 2.14. This similarity in the rate coefficients or cross-sections for collisions with *para*- and *ortho*-H_2 has also been observed for other molecular ions, e.g. N_2H^+ (Balança et al. 2020), SH^+ (Dagdigian 2019), CF^+ (Desrousseaux et al. 2019), C_3N^- (Lara-Moreno, Stoecklin & Halvick 2019), C_6H^- (Walker et al. 2017), CN^- (Kłos & Lique 2011), and HC_3N (Wernli

Downloaded from https://academic.oup.com/mnras/article/497/4/4276/5881339 by guest on 28 September 2020

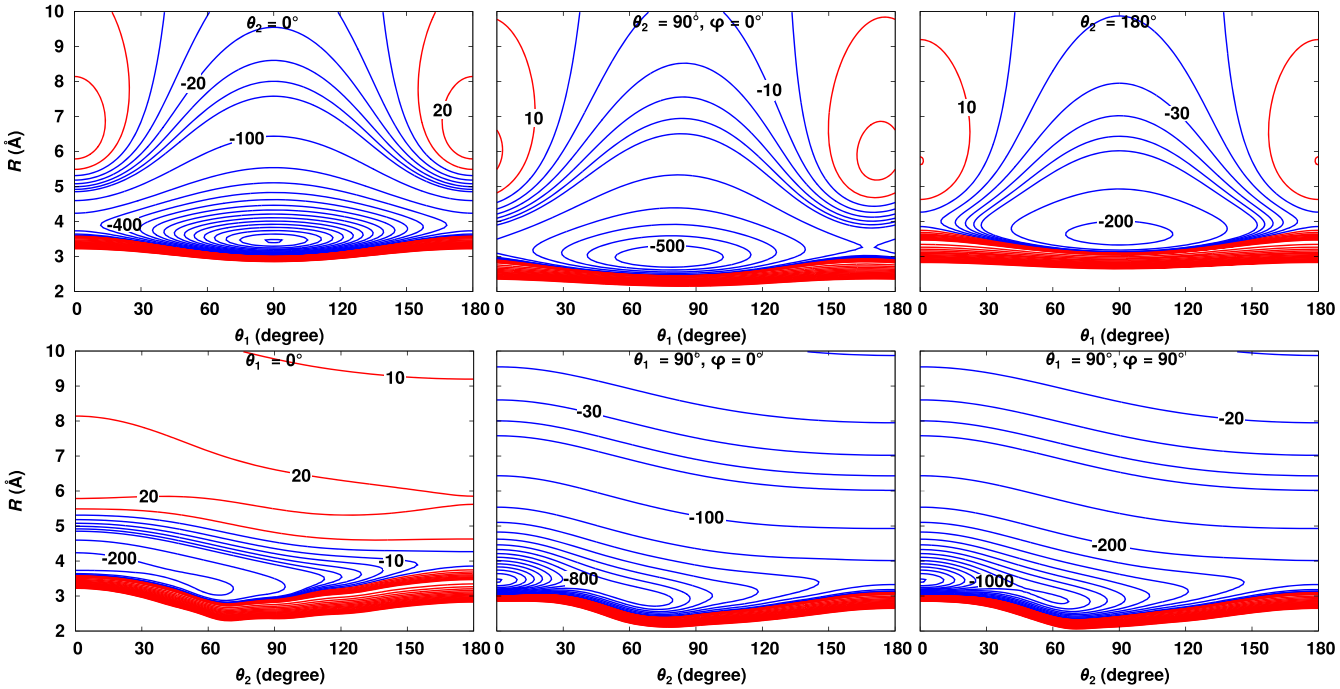

Figure 3. Contour plots of the HCO$^+$ + H$_2$ interaction PES at several angular configurations (negative energies are represented in blue).

Table 2. Rotational de-excitation rate coefficients ($\times 10^{-10}$ cm^3 molecule^{-1} s^{-1}) of HCO$^+$ by collision with *para*-H$_2$ (p-H$_2$) and *ortho*-H$_2$ (o-H$_2$) at several temperatures. Rate coefficients for HCO$^+$ + *para*-H$_2$ from (Monteiro 1985) (M85), (Flower 1999) (F99), (Yazidi et al. 2014) (Y14), and (Massó & Wiesenfeld 2014) (M14) are also included. A full set of rotational de-excitation rate coefficients of HCO$^+$ by collisions with *para*- and *ortho*-H$_2$ can be found in the supplementary materials.

T	M85	F99	Y14	M14	This work p-H2	This work o-H2	F99	Y14	This work p-H2	This work o-H2
1 → 0							5 → 2			
10	2.50	2.64	2.39	2.30	2.48	2.74	2.10	2.24	2.19	2.16
30	2.10	2.14	2.04	2.00	2.09	2.24	1.90	1.90	1.93	1.92
100	–	1.85	2.00	–	1.96	2.09	1.70	1.46	1.51	1.49
2 → 0							5 → 3			
10	1.50	1.35	1.69	–	1.51	1.55	3.00	3.26	3.38	3.38
30	1.20	1.13	1.32	–	1.25	1.20	2.80	2.86	2.94	2.95
100	–	0.88	0.91	–	0.89	0.87	2.60	2.23	2.30	2.33
2 → 1							5 → 4			
10	4.50	3.93	4.40	–	4.10	4.63	4.20	3.74	3.53	3.91
30	3.70	3.67	3.67	–	3.56	3.87	4.00	3.62	3.55	3.82
100	–	3.32	3.33	–	3.31	3.47	4.00	3.70	3.65	3.91
3 → 0							10 → 7			
10	0.83	1.00	0.97	–	0.91	0.89	2.10	1.87	1.96	1.98
30	0.63	0.84	0.73	–	0.68	0.76	1.90	1.80	1.86	1.88
100	–	0.63	0.52	–	0.48	0.54	1.80	1.65	1.68	1.68
3 → 1							10 → 8			
10	2.90	2.66	2.80	–	2.79	2.97	2.60	2.41	2.36	2.47
30	2.30	2.32	2.26	–	2.23	2.32	2.40	2.39	2.35	2.38
100	–	1.80	1.68	–	1.67	1.71	2.30	2.26	2.24	2.26
3 → 2							10 → 9			
10	4.00	4.48	4.49	–	4.67	4.78	2.80	2.50	2.51	2.50
30	3.90	4.17	4.03	–	4.07	4.20	3.20	2.59	2.53	2.65
100	–	3.90	3.84	–	3.79	3.89	3.70	2.87	2.83	3.09

et al. 2007). Two explications for this behaviour have been given. Walker et al. (2017) pointed out that the similarities come from the fact that the effects in the long-range interaction outweigh those from the short range. However, in the study of C_3N^- + H_2, Lara-Moreno et al. (2019) found that the similarities decrease at low temperatures, where the long range dominates the dynamics. These authors showed that the short-range interaction appears to be dominated by the attractive isotropic A^0_{00} term that gives non-zero contributions in the matrix element of the potential for collisions involving both *para*-$H_2(j = 0)$ and *ortho*-$H_2(j = 1)$ (Lara-Moreno

Downloaded from https://academic.oup.com/mnras/article/497/4/4276/5881339 by guest on 28 September 2020

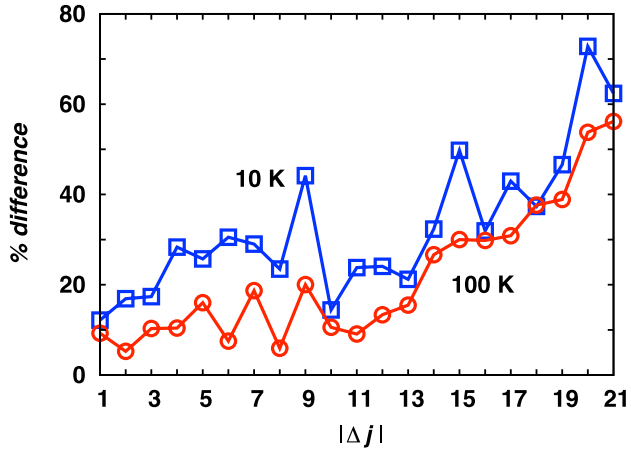

Figure 4. Maximum percentage difference between the rate coefficients of HCO^+ by collision with *ortho*- and *para*-H_2 at different $|\Delta j|$ for $T = 10$ and 100 K.

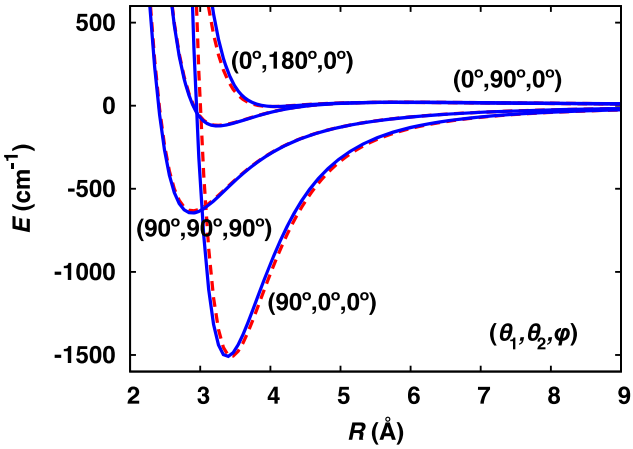

Figure 5. PES for $DCO^+ + H_2$ (solid lines) at several geometries. The same cuts for the $HCO^+ + H_2$ complex are also included (dashed lines).

et al. 2019). The case of $HCO^+ + H_2$ is particular because the similarities are observed at both the lower and larger temperatures analysed, which can be explained by a combination of the arguments mentioned above, one acting at low temperatures and the other at high temperatures.

A small modification in the PES allows studying the collision of $DCO^+ + H_2$. The coordinates for $DCO^+ + H_2$ differ from those for $HCO^+ + H_2$ only by small displacement of the centre of mass in the DCO^+ molecules. The old coordinates were expressed as a function of the new one from geometrical considerations (Sultanov, Guster & Adhikari 2012), and a new grid of energies was generated and fitted using the same expression 1. The influence of this correction in the PES is small (see Fig. 5), and it is not expected to play an essential role in the dynamics.

The modified surface was employed in close-coupling calculations. The same parameters used in the dynamics for $HCO^+ + H_2$ were employed. The only different data used were the mass of deuterium and the rotational constant of DCO^+ named $B_{DCO^+} = 1.201$ cm^{-1} (Caselli & Dore 2005).

Fig. 6 shows the rotational de-excitation rate coefficients for the collision of DCO^+ with *para*- and *ortho*-H_2 from $j = 5$. The difference between both sets of rate coefficients is also very small,

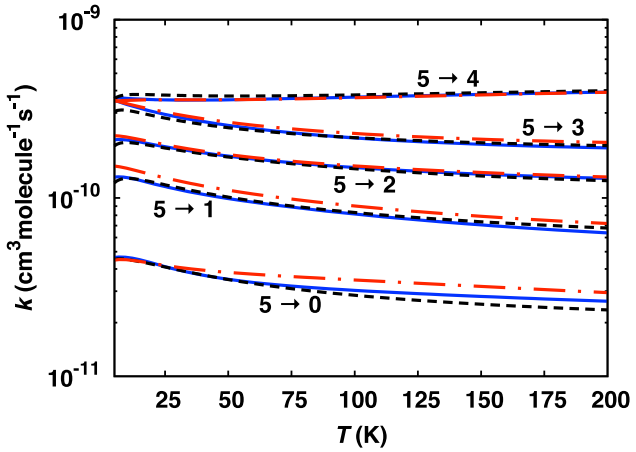

Figure 6. De-excitation rate coefficients of DCO^+ with *para*-H_2 (solid lines) and *ortho*-H_2 (dashed lines) from $j = 5$. The rate coefficients for $HCO^+ + para$-H_2 (dash–dotted line) are also included.

like in the case of HCO^+, as expected due to the very small differences between both PESs. The rate coefficients for $HCO^+ + para$-H_2 are also included in Fig. 6, and the differences with DCO^+ are very small. For all the rate coefficients computed in this work, the ratio between the $DCO^+ + para$-H_2 and $HCO^+ + para$-H_2 rate coefficients varies from 0.44 up to 1.98. Using the $HCO^+ + para$-H_2 rate coefficients for reproducing those of $DCO^+ + H_2$ then appears to be approximately valid. The $DCO^+ + para$-H_2 rate coefficients that can be found in the supplementary materials should, however, be preferred for analysing the DCO^+ observations as these differences are not completely negligible.

4 SUMMARY

A new PES for the $HCO^+ + H_2$ complex at the CCSD(T)-F12a/aug-cc-pVTZ level of theory was developed in this work. Close-coupling calculations were performed using this PES. A new set of rate coefficients for $HCO^+ + para$-H_2 was reported and compared with previous calculations. Furthermore, the first set of rate coefficients for a large number of rotational states of HCO^+ in collision with *ortho*-H_2 was determined. Similarities between the rate coefficients for collisions with *para*- and *ortho*-H_2 were found. The collision of DCO^+ with H_2 was also investigated, and a set of rate coefficients for $DCO^+ + para$-H_2 was also reported. These rate coefficients are very close to those for $HCO^+ + H_2$, which justifies the use of the latter to analyse the observations of the DCO^+.

ACKNOWLEDGEMENTS

Computer time for this study was provided by the Mésocentre de Calcul Intensif Aquitain, which is the computing facility of Université de Bordeaux et Université de Pau et des Pays de l'Adour. We acknowledge the support from the ECOS-SUD-CONICYT project number C17E06 (Programa de Cooperación Científica ECOS-CONICYT ECOS170039).

DATA AVAILABILITY

The data underlying this article are available in the article and in its online supplementary material.

Downloaded from https://academic.oup.com/mnras/article/497/4/4276/5881339 by guest on 28 September 2020

REFERENCES

Balança C., Scribano Y., Loreau J., Lique F., Feautrier N., 2020, MNRAS, 495, 2524
Bieske E., Nizkorodov S., Bennett F., Maier J., 1995, J. Chem. Phys., 102, 5152
Boys S. F., Bernardi F. D., 1970, Mol. Phys., 19, 553
Buffa G., 2012, MNRAS, 421, 719
Buffa G., Dore L., Meuwly M., 2009, MNRAS, 397, 1909
Buhl D., Snyder L. E., 1970, Nature, 228, 267
Cabrera-González L., Páez-Hernández D., Denis-Alpizar O., 2020, MNRAS, 494, 129
Caselli P., Dore L., 2005, A&A, 433, 1145
Caselli P., Walmsley C. M., Terzieva R., Herbst E., 1998, ApJ, 499, 234
Dagdigian P. J., 2019, MNRAS, 487, 3427
Denis-Alpizar O., Stoecklin T., Halvick P., 2014, J. Chem. Phys., 140, 084316
Denis-Alpizar O., Stoecklin T., Halvick P., 2015, MNRAS, 453, 1317
Desrousseaux B., Quintas-Sanchez E., Dawes R., Lique F., 2019, J. Phys. Chem. A, 123, 9637
Dubernet M. et al., 2013, A&A, 553, 50
Dunning T. H., 1989, J. Chem. Phys., 90, 1007
Dutrey A. et al., 2014, in Beuther H., Klessen R. S., Dullemond C. P., Henning T., eds, Protostars and Planets VI. Univ. Arizona Press, Tucson, AZ, USA, p. 317
Flower D., 1999, MNRAS, 305, 651
Guillon G., Stoecklin T., Voronin A., Halvick P., 2008, J. Chem. Phys., 129, 104308
Halkier A., Klopper W., Helgaker T., Jørgensen P., Taylor P. R., 1999, J. Chem. Phys., 111, 9157
Ho T. S., Rabitz H., 1996, J. Phys. Chem., 104, 2584
Huang J. et al., 2017, ApJ, 835, 231
Jankowski P., Szalewicz K., 1998, J. Chem. Phys., 108, 3554
Kłos J., Lique F., 2011, MNRAS, 418, 271
Knizia G., Adler T. B., Werner H., 2009, J. Chem. Phys., 130, 054104
Kraemer W., Diercksen G., 1976, ApJ, 205, L97
Lara-Moreno M., Stoecklin T., Halvick P., 2019, MNRAS, 486, 414
Li H., Hirano T., Amano T., Le Roy R. J., 2008, J. Chem. Phys., 129, 244306
Lique F., Kalugina Y., Chefdeville S., van de Meerakker S. Y. T., Costes M., Naulin C., 2014, A&A, 567, A22
Lucas R., Liszt H., 1996, A&A, 307, 237
Manolopoulos D. E., 1988, PhD thesis, Univ. Cambridge
Massó H., Wiesenfeld L., 2014, J. Chem. Phys., 141, 184301
Monteiro T., 1985, MNRAS, 214, 419
Pagani L., Bourgoin A., Lique F., 2012, A&A, 548, L4
Schöier F. L., van der Tak F. F. S., van Dishoeck E. F., Black J. H., 2005, A&A, 432, 369
Soldán P., Hutson J. M., 2000, J. Chem. Phys., 112, 4415
Stoecklin T., Denis-Alpizar O., Halvick P., Dubernet M.-L., 2013, J. Chem. Phys., 139, 124317
Stoecklin T., Faure A., Jankowski P., Chefdeville S., Bergeat A., Naulin C., Morales S., Costes M., 2017, Phys. Chem. Chem. Phys., 19, 189
Sultanov R. A., Guster D., Adhikari S. K., 2012, AIP Adv., 2, 012181
Walker K. M., Lique F., Dumouchel F., Dawes R., 2017, MNRAS, 466, 831
Werner H.-J., Knowles P. J., Knizia G., Manby F. R., Schütz M., 2012, WIREs Comput. Mol. Sci., 2, 242
Wernli M., Wiesenfeld L., Faure A., Valiron P., 2007, A&A, 464, 1147
Woods R., 1988, Phil. Trans. R. Soc. A, 324, 141
Yazidi O., Ben Abdallah D., Lique F., 2014, MNRAS, 441, 664

SUPPORTING INFORMATION

Supplementary data are available at *MNRAS* online.

rate-oh2-hcop.dat
rate-ph2-dcop.dat
rate_ph2-hcop.dat

Please note: Oxford University Press is not responsible for the content or functionality of any supporting materials supplied by the authors. Any queries (other than missing material) should be directed to the corresponding author for the article.

This paper has been typeset from a TEX/LATEX file prepared by the author.

Downloaded from https://academic.oup.com/mnras/article/497/4/4276/5881339 by guest on 28 September 2020